

Selected Paper

Resonance Raman Spectra of β-Diketiminatocopper(II) Complexes

Tomoko Miyazaki, Chizu Shimokawa,† Toshio Matsushita, Shinobu Itoh,†† and Junji Teraoka*

Department of Chemistry, Graduate School of Science, Osaka City University,
3-3-138 Sugimoto, Sumiyoshi-ku, Osaka 558-8585

Received April 28, 2010; E-mail: teraoka@sci.osaka-cu.ac.jp

Resonance Raman spectra are measured for copper(II) complexes ([Cu(^{R}L)$_2$]) using a series of β-diketiminate ligands (L) carrying different α-substituents (R = Me, H, CN, and NO_2), and quantum chemical calculations based on density functional theory (DFT) are carried out in order to derive the force fields of the copper(II) complexes. The complexes show characteristic ν_{sym}(Cu–N) frequencies, reflecting the relatively long distance of Cu–N bond in [Cu(^{CN}L)$_2$]. No obvious correlations were found for the other Raman bands between frequencies and the electron-withdrawal properties of the ligands. Resonance Raman profiles for [Cu(^{Me}L)$_2$] and [Cu(^{H}L)$_2$] suggest that two intense electronic absorption bands should be assigned to a charge-transfer transition accompanied by changing the Cu–N bond length and $\pi^* \leftarrow \pi$ transition by lengthening the C_β–N bond with the aid of theoretical calculations. It is found that the complexes, [Cu(^{CN}L)$_2$] and [Cu(^{NO_2}L)$_2$] with electron-withdrawing ligands, which yield only one strong absorption band around the visible region, show mainly $\pi^* \leftarrow \pi$ transition by lengthening the C_β–N bond.

β-Diketiminate derivatives have been applied as monomeric bidentate ligands to a wide variety of transition metal, main group element, and lanthanide complexes.[1] A number of recent efforts have been focused on the substituents effects of the carbon framework in order to control the reactivity of β-diketiminate complexes.[2–4] For these studies, a series of β-diketiminate ligands carrying a different C_α substituent (R = Me, H, CN, and NO_2) have been employed for the synthesis of copper(II) complexes[5] (Figure 1). The crystal structures of bis(β-diketiminato)copper(II) complexes ([Cu(^{R}L)$_2$]), except for [Cu(^{Me}L)$_2$], have been determined by X-ray crystallographic analysis, and indicate that they exhibit distorted tetrahedral geometries. The electronic nature of the substituent R affects neither the dihedral angles between the two coordination planes nor the mean values of the Cu–N bond length.[5] It was pointed out that smaller hyperfine parameter $A_\parallel$ values of an unpaired d-electron coupled with the nucleus spin of the copper atom, as compared to that of square-planar copper(II) complexes, were characteristic features of tetrahedrally distorted complexes, which indicates that the complexes maintain similar structures in solution as in the crystal. However, it was mentioned that the $g_\parallel$ values were correlated to the electron-donating nature of R, and the absorption spectra are also sensitive to the nature, in particular, the strong absorption bands ($\varepsilon > 10^4\,M^{-1}\,cm^{-1}$) below 500 nm that could be attributed to $\pi^* \leftarrow \pi$ transitions of the β-diketiminate ligands shift toward longer wavelength as the electron-donating nature of R increases as well as the shifts toward longer wavelength of the d ← d transition band in the near-IR region.[5]

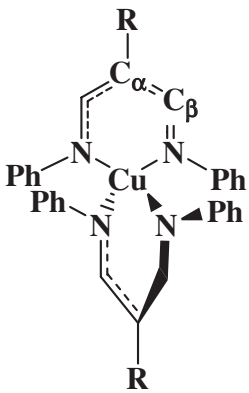

[Cu(^{R}L)$_2$]	R
[Cu(^{Me}L)$_2$]	Me
[Cu(^{H}L)$_2$]	H
[Cu(^{CN}L)$_2$]	CN
[Cu(^{NO_2}L)$_2$]	NO_2

Figure 1. Schematic molecular structure of bis(β-diketiminato)copper(II) complexes and labeling of atoms. The abbreviation is [Cu(^{R}L)$_2$] with substituents of R at C_α.

It was also reported that more than two absorption bands are observed in the 400 to 500 nm region for [Cu(^{H}L)$_2$] and [Cu(^{Me}L)$_2$] but not for [Cu(^{CN}L)$_2$] and [Cu(^{NO_2}L)$_2$].[5]

It turns out that structural differences in the core of the complexes with such ligands can be detected in solution via ESR and electronic absorption spectra. However, it is difficult on the basis of these observations to estimate differences in structural parameters such as bond lengths and angles. Resonance Raman (RR) scattering is a powerful tool to investigate the molecular structure of copper complexes;[2,6–8] vibrational frequencies are essential for estimating the bond character in the Cu–O unit in copper–oxygen complexes. Moreover, the RR intensity profile for a certain band, which is the intensity behavior as a function of excitation wavelengths, is useful to investigate the symmetry of the molecule in the electronic excited states. Therefore, this technique is useful to study differences in the bond lengths and bond angles as well as the torsional angles of the ligand planes in [Cu(^{R}L)$_2$].

† Present address: School of Medicine, Kurume University, Kurume 830-0011

†† Present address: Department of Material and Life Science, Graduate School of Engineering, Osaka University, 2-1 Yamada-oka, Suita, Osaka 565-0871

Published on the web October 5, 2010; doi:10.1246/bcsj.20100124

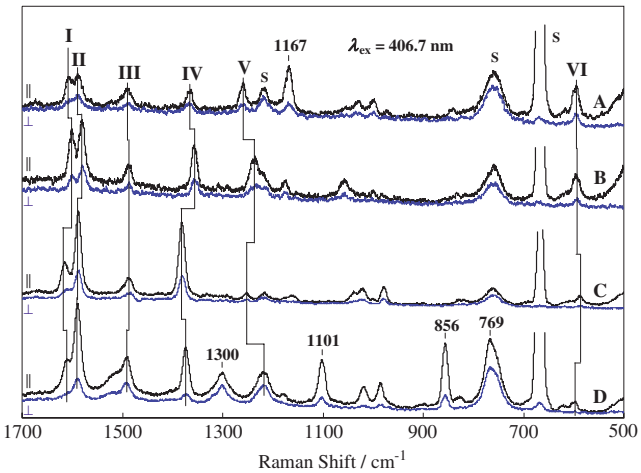

Figure 2. Polarized RR spectra in the 500–1700 cm^{-1} region for (A) [Cu(^{Me}L)$_2$], (B) [Cu(^{H}L)$_2$], (C) [Cu(^{CN}L)$_2$], and (D) [Cu(^{NO_2}L)$_2$] in $CHCl_3$, with parallel (∥) and perpendicular (⊥) components. Spectra were recorded using 406.7 nm excitation, 7.0 mW laser power, and 4 cm^{-1} slit widths. S indicates the solvent Raman band. The Raman bands, which have similar vibration modes, are named I–VI. The Raman band at 769 cm^{-1} is overlapped with the solvent band but obviously seen in Figure 6A where the sample is dissolved in THF.

The purpose of the present study was to evaluate the RR spectra of four different types of bis(β-diketiminato)copper(II) complexes, [Cu(^{R}L)$_2$], in solution with the aid of vibrational frequency calculations in order to investigate the molecular structures and elucidate the electronic absorption bands around the visible-to-UV region.

Results and Discussion

Polarized RR spectra of the copper(II) complexes [Cu(^{Me}L)$_2$], [Cu(^{H}L)$_2$], [Cu(^{CN}L)$_2$], and [Cu(^{NO_2}L)$_2$] in the 500 to 1700 cm^{-1} region with excitation at 406.7 nm are shown in Figure 2. The spectra of [Cu(^{R}L)$_2$] are compared from the top (A) to the bottom (D) with decreasing electron-donating nature of R, where R = Me, H, CN, and NO_2. Upon excitation at 406.7 nm, almost all the Raman bands have small values of depolarization ratio with the exception of a Raman band at 1300 cm^{-1} for [Cu(^{NO_2}L)$_2$] which has a value of 0.7. Several Raman bands, characteristic of the substituents R of the complexes, are observed at 1167 cm^{-1} for [Cu(^{Me}L)$_2$] and at 1300, 1101, 856, and 769 cm^{-1} for [Cu(^{NO_2}L)$_2$]. The Raman band at 1300 cm^{-1} has a width of 32 cm^{-1} that is roughly twice as wide as those for the bands observed at 1101 and 856 cm^{-1}. A vibrational mode due to ν(C–N) for [Cu(^{CN}L)$_2$] gives rise to a characteristic IR absorption band at 2205 cm^{-1} (not shown here). The spectral patterns, however, are similar to each other in which a set of Raman bands are observed, named Raman bands I–VI in the order of the Raman shifts. The frequencies are listed in Table 1 together with those of the other characteristic Raman modes for the complexes. No simple and monotonic frequency shifts are found in any of the Raman bands with changes in the electron-donating nature of the substituents, R. However, there are some common tendencies for the Raman frequencies. The Raman bands I, IV, and V show prominent zigzag shifts, with almost 30 cm^{-1} deviation, especially Raman bands IV and V. A few shifts are observed for Raman bands II and III as well. There are a few less resonance-enhanced Raman bands around 1000 cm^{-1} but it is difficult to find Raman bands that correspond with one another.

Normal mode analysis for complexes is required in order to interpret the observed frequency shifts and spectral behavior in different solvents and with different excitation wavelengths. The normal mode analysis is carried out on the basis of the DFT method. The spin multiplicity is a *doublet* in the electronic ground state since the copper(II) complexes possess an odd number of electrons. There are 98a and 97b vibrations for [Cu(^{Me}L)$_2$] under C_2 symmetry, 44a, 43b_1, 45b_2, and 45b_3 vibrations for [Cu(^{H}L)$_2$] under D_2 symmetry, 45a, 44b_1, 47b_2, and 47b_3 vibrations for [Cu(^{CN}L)$_2$] under D_2 symmetry, and 47a, 46b_1, 48b_2, and 48b_3 vibrations for [Cu(^{NO_2}L)$_2$] under D_2 symmetry. Here, it is assumed that the three complexes with D_2 symmetry have a twofold principal axis through the atoms of C_α–Cu–C_α (Figure 1), while the [Cu(^{Me}L)$_2$] complex has its own C_2 axis perpendicular to the C_2 axis for the complexes with D_2 symmetry. X-ray crystallography supports such symmetries under which two phenyl groups bound to N atoms in one ligand are almost indistinguishable through the rotation with respect to the C_2 axis. Consequently, these symmetries were adopted for the DFT calculations. The DFT vibrational frequencies were scaled using a single scaling factor of 0.9582 that will be mentioned in the experimental section. The calculated Raman bands are listed along with the observed ones in Table 1, and their frequencies and depolarization ratios are compared. Nearly all of the observed Raman bands are *polarized* with the exception of one band at 1300 cm^{-1} for [Cu(^{NO_2}L)$_2$]. A Raman band at 1217 cm^{-1} for [Cu(^{NO_2}L)$_2$] is *polarized* although the apparent polarization ratio is estimated to be 0.7 as shown in Table 1, since the band overlaps with a strong *depolarized* Raman band due to the solvent. Thus, all vibrational modes belonging to A species in each point group are picked from the calculated ones. The vibrational modes associated with the phenyl rings are eliminated as candidates for the observed Raman bands since they are not resonance-enhanced upon visible excitation, which is supported by the fact that the dihedral angle between the ligand constructed by N–C_β–C_α–C_β–N atoms and the phenyl ring is ca. 40 degrees and they are not in the same plane.[5] Note that the stretching vibration of N–C_ϕ, however, is still resonance-enhanced. As a result, Raman bands I and II are assigned mainly to both ν(C_α–C_β) and ν(C_β–N), but ν(C_α–C_β) is dominant for band I and ν(C_β–N) is dominant for band II. The Raman band III is assigned to ν(N–C_ϕ) and the frequencies of Raman bands II and III are independent of the type of substituents. Raman band IV is assigned to ν(C_β–N) and ν(C_α–R), Raman band V to ν(N–C_ϕ) and ν(C_α–R) and Raman band VI to ν(Cu–N). Details are presented in Table 1. The differences in frequency ($\Delta = \nu_{obs} - \nu_{calc}$) and the percentages ($100\Delta/\nu_{obs}$) are also shown in the table and the discrepancies are less than 1% for most bands. For instance, Raman band IV gives rise to 1365 (calcd 1364), 1355 (calcd 1354), 1380 (calcd 1374), and 1372 cm^{-1} (calcd 1364) for [Cu(^{Me}L)$_2$], [Cu(^{H}L)$_2$], [Cu(^{CN}L)$_2$], and [Cu(^{NO_2}L)$_2$], respectively. As a consequence, even a zigzag

Table 1. Comparison of Observed and Calculated Frequencies for RR Vibrational Modes of $[Cu(^{Me}L)_2]$, $[Cu(^{H}L)_2]$, $[Cu(^{CN}L)_2]$, and $[Cu(^{NO_2}L)_2]$ in $CHCl_3$

Observed			Calculated				
Band	Freq./cm^{-1}	ρ	Mode	Freq./cm^{-1}	Δ[a]/cm^{-1}	%[b]	Displacement[c]
$[Cu(^{Me}L)_2]$							
I	1605	0.32	ν_{16}	1597	8	0.5	$C_\beta N - C_\alpha C_\beta$
II	1587	0.46	ν_{18}	1576	11	0.7	$C_\beta N - C_\alpha C_\beta$
III	1488	0.44	ν_{22}	1482	6	0.4	NC_ϕ
IV	1365	0.51	ν_{30}	1364	1	0.1	$C_\beta N - C_\alpha Me$
V	1260	0.37	ν_{36}	1240	20	1.6	$NC_\phi + C_\alpha Me$
R[d]	1167	0.29	ν_{42}	1144	23	2.0	$C_\alpha Me$
VI	596	0.33	ν_{72}	596	0	0.0	CuN
$[Cu(^{H}L)_2]$							
I	1599	0.32	ν_8	1593	6	0.4	$C_\beta N - C_\alpha C_\beta$
II	1579	0.42	ν_9	1569	10	0.6	$C_\beta N - C_\alpha C_\beta$
III	1485	0.51	ν_{11}	1483	2	0.1	NC_ϕ
IV	1355	0.37	ν_{13}	1354	1	0.1	$C_\beta N$
V	1236	0.37	ν_{16}	1215	21	1.7	NC_ϕ
VI	595	0.29	ν_{33}	595	0	0.0	CuN
$[Cu(^{CN}L)_2]$							
R	2205			2183	22	1.0	CN
I	1613	0.34	ν_8	1600	13	0.8	$C_\beta N - C_\alpha C_\beta$
II	1586	0.35	ν_9	1575	11	0.7	$C_\beta N - C_\alpha C_\beta$
III	1485	0.38	ν_{11}	1482	3	0.2	NC_ϕ
IV	1380	0.34	ν_{13}	1374	6	0.4	$C_\beta N - C_\alpha CN - CN$
V	1252	0.50	ν_{16}	1233	19	1.5	$NC_\phi + C_\alpha CN - CN$
VI	587	0.27	ν_{34}	584	3	0.5	CuN
$[Cu(^{NO_2}L)_2]$							
I	1609	0.25	ν_7	1596	13	0.8	$C_\beta N$
II	1587	0.24	ν_8	1572	15	0.9	$C_\beta N$
III	1490	0.50	ν_{10}	1483	7	0.5	NC_ϕ
IV	1372	0.19	ν_{12}	1364	8	0.6	$C_\beta N - C_\alpha NO_2$
R	1300	0.71		1346	−46	3.4	$^{as}NO_2$, $C_\alpha C_\beta$
V	1217	0.70	ν_{15}	1229	−12	1.0	$C_\alpha NO_2 - NO_2$
R	1101	0.22	ν_{20}	1068	33	3.0	$C_\alpha NO_2 + NO_2$
R	856	0.24	ν_{29}	819	37	4.3	δNO_2
R	769	0.58	ν_{31}	729	40	5.2	δNO_2
VI	598	0.19	ν_{34}	597	1	0.2	CuN

a) Frequency difference between observed and calculated. b) $(100\Delta/\nu_{obs})$. c) $C_\beta N$ means $\nu(C_\beta\text{–}N)$ and the $\pm$ signs signify in-phase or out-of-phase for the stretching vibrations. d) A characteristic Raman band for each complex.

shift pattern is clearly reproduced by the DFT calculations. The zigzag behavior probably results from alteration of the degree of couplings between local vibrational modes caused mainly by mass difference of the substituents. In fact, $[Cu(^{H}L)_2]$ gives rise to different frequencies, because of the lack of vibrational couplings between the ligand and a light substituent such as a hydrogen atom. Therefore, frequencies of skeletal vibrational modes of the complexes basically show a downshift with increasing mass, such as $Me < CN < NO_2$ except for $[Cu(^{H}L)_2]$.

The characteristic Raman band VI, which is assigned to the totally symmetric stretching mode of the metal to four ligand nitrogen atoms, gives rise to 596 (calcd 596), 595 (calcd 595), 587 (calcd 584), and 598 cm^{-1} (calcd 597) for $[Cu(^{Me}L)_2]$, $[Cu(^{H}L)_2]$, $[Cu(^{CN}L)_2]$, and $[Cu(^{NO_2}L)_2]$), respectively, and these calculated frequencies are in fair agreement with the observed values with deviations of less than 0.5%. This mode is in the core part of the complexes and it seems that this frequency matching occurs mainly due to the specific vibrational mode which is less affected by intermolecular interactions such as solvent effects. Therefore, it is not necessarily meaningless to discuss only the 10 cm^{-1} (2%) shift for the Raman band VI for $[Cu(^{CN}L)_2]$ compared to the others. The force constant of Raman band VI for $[Cu(^{CN}L)_2]$ is weakened by ca. 4% compared to $[Cu(^{NO_2}L)_2]$ which is calculated as follows:

$$k([Cu(^{CN}L)_2])/k([Cu(^{NO_2}L)_2]) = (587/598)^2 \quad (1)$$

Table 2. Comparison of Observed and Calculated Bond Lengths (Å), Angles (degree), and Angles of Least-Square Planes (degree) of $[Cu(^{Me}L)_2]$, $[Cu(^{H}L)_2]$, $[Cu(^{CN}L)_2]$, and $[Cu(^{NO_2}L)_2]$

	$[Cu(^{Me}L)_2]$	$[Cu(^{H}L)_2]$		$[Cu(^{CN}L)_2]$		$[Cu(^{NO_2}L)_2]$	
	Calcd	Obsd[a)]	Calcd	Obsd[a)]	Calcd	Obsd[a)]	Calcd
Cu–N	1.973	1.951	1.977	1.959	1.975	1.952	1.977
N–C_β	1.339	1.320	1.338	1.308	1.328	1.307	1.324
N–C_ϕ	1.428	1.416	1.428	1.430	1.434	1.426	1.436
C_α–C_β	1.404	1.395	1.400	1.407	1.416	1.404	1.410
N–Cu–N	95.60	96.10	96.50	95.40	95.90	96.21	95.80
Cu–N–C_β	122.7	122.9	122.1	123.8	123.0	123.6	123.2
Cu–N–C_ϕ	119.0	117.8	119.3	117.9	118.7	118.0	118.7
C_β–N–C_ϕ	119.0	119.2	118.5	118.1	118.2	118.3	118.1
C_β–C_α–C_β	124.2	126.7	126.6	126.4	125.6	128.3	127.4
N–C_β–C_α	127.4	125.6	126.4	125.3	126.2	124.1	125.2
Angle of planes[b)]	65.98	63.68	65.78	62.48	65.26	62.03	64.42
C_α–C(Me)	1.522	—	—	—	—	—	—
C_α–C(CN)	—	—	—	1.437	1.428	—	—
C–N(CN)	—	—	—	1.140	1.178	—	—
C_α–N(NO_2)	—	—	—	—	—	1.438	1.442
N–O(NO_2)	—	—	—	—	—	1.235	1.276
O–N–O(NO_2)	—	—	—	—	—	122.5	122.5

a) X-ray crystallographic data from Ref. 5. b) Angles of planes mean dihedral angles of two ligand's planes.

where k are the force constants. The mean bond lengths of Cu–N are revealed by X-ray analysis to be 1.951, 1.959, and 1.952 Å for $[Cu(^{H}L)_2]$, $[Cu(^{CN}L)_2]$, and $[Cu(^{NO_2}L)_2]$, respectively.[5] The relatively long distance of Cu–N in $[Cu(^{CN}L)_2]$ is consistent with the 4% decrease in the force constant estimated by Raman measurements. However, how the Cu–N force constant is weakened in $[Cu(^{CN}L)_2]$ with CN substituents has not yet been revealed.

Neither the frequencies of Raman band V nor any of the Raman bands involving vibrations of substituents R are well-reproduced by the DFT calculations, whose discrepancy is 1.5% for Raman band V and more than that for the R-related characteristic bands. The ν_{42} for $[Cu(^{Me}L)_2]$ observed at 1167 cm^{-1} is assigned mainly to the C_α–Me stretching but varies from the calculated value by 23 cm^{-1} (2%). A similar discrepancy was also found for the C–N stretching frequencies for $[Cu(^{CN}L)_2]$ of 22 cm^{-1} (1%) as an IR absorption band. For $[Cu(^{NO_2}L)_2]$, there are significant differences for $\nu_{as}(NO_2)$ at 1300 cm^{-1}, $\nu(C_\alpha$–$NO_2)$ at 1101 cm^{-1}, and $\delta(NO_2)$s at 856 and 769 cm^{-1}, by −46 (−3.4%), +33 (3%), +37 (4.3%), and +40 cm^{-1} (5.2%), respectively. The disparities cannot be solved by manipulating scaling factors and frequency calculation based on DFT has to be appropriately improved for the molecule with several resonance structures such as $–NO_2$. Such a development has not been adopted here since the assignments of vibrational modes are basically completed at this stage. Optimized structural parameters such as bond lengths and angles for $[Cu(^{R}L)_2]$ are summarized together with the X-ray analyses data in Table 2. Optimized data are generally in fair agreement with the experimental data but differences are prominent especially for the bond lengths of substituents R, which is consistent with the frequency disparities discussed above.

The four sets of RR spectra shown in Figure 2 can now be compared from a different point of view, that is, resonance enhancements of the Raman intensity. All of the RR spectra excited at 406.7 nm have corresponding Raman bands I to VI in common and can be classified into two groups, group A consisting of a member of $[Cu(^{Me}L)_2]$ and $[Cu(^{H}L)_2]$, and group B consisting of $[Cu(^{CN}L)_2]$ and $[Cu(^{NO_2}L)_2]$ in terms of resonance enhancement effects. Raman bands I, V, and VI are resonance-enhanced in group A while Raman bands II and IV are resonance-enhanced in group B. The resonance Raman intensity pattern is strongly related to the symmetry of an intermediate electronic excited state in the resonance Raman process. Strong electronic absorption bands that could be assigned to $\pi^* \leftarrow \pi$ transitions of the ligands are at 370 nm for $[Cu(^{NO_2}L)_2]$, 388 nm for $[Cu(^{CN}L)_2]$, 400 nm with a shoulder at 445 nm for $[Cu(^{H}L)_2]$, and a couple of bands at 410 and 450 nm for $[Cu(^{Me}L)_2]$ with absorption coefficients ($\varepsilon = 17000$–47000). As mentioned before, the absorption maxima shift to longer wavelengths as the nature of electron donation of the substituents increases. The bands of $[Cu(^{Me}L)_2]$ and $[Cu(^{H}L)_2]$ belonging to group A are graphically divided by two bands, as shown in the inset figures in Figures 3 and 4, where the absorption bands are named Abs-band I (at shorter wavelength) and II (at longer wavelength). The molar absorption coefficients are 10000 ($[Cu(^{NO_2}L)_2]$), 28000 ($[Cu(^{CN}L)_2]$), 35000 ($[Cu(^{H}L)_2]$), and 27000 ($[Cu(^{Me}L)_2]$) $M^{-1}\,cm^{-1}$ at 406.7 nm that is the wavelength of the excitation laser. The RR spectra of $[Cu(^{Me}L)_2]$ and $[Cu(^{H}L)_2]$ are considered to be resonant with the electronic excited states related to Abs-band I, giving rise to different patterns of spectra from those obtained for group B which has a single absorption band. Consequently, the absorption bands for group B have show dissimilar transition compared to Abs-band I of group A. It is interesting to observe the RR spectra of the complexes belonging to group A on longer wavelength excitation resonant with Abs-band II in order to correctly understand the nature of the absorption bands.

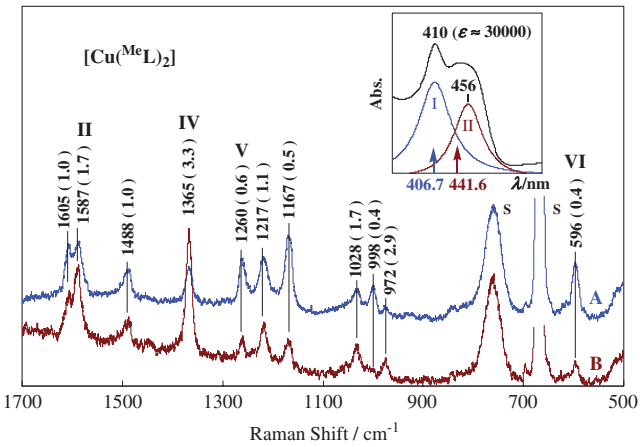

Figure 3. RR spectra of $[Cu(^{Me}L)_2]$ in $CHCl_3$ obtained in the 500–1700 cm^{-1} region using 406.7 nm excitation, 7.0 mW (A) and 441.6 nm excitation, 5.9 mW (B) with 4 cm^{-1} slit width. The sample concentration is the same for A and B. S indicates the solvent Raman band. The relative intensities (441.6/406.7 nm) of Raman bands are shown in parentheses. Inset: Absorption spectrum of $[Cu(^{Me}L)_2]$ in $CHCl_3$.

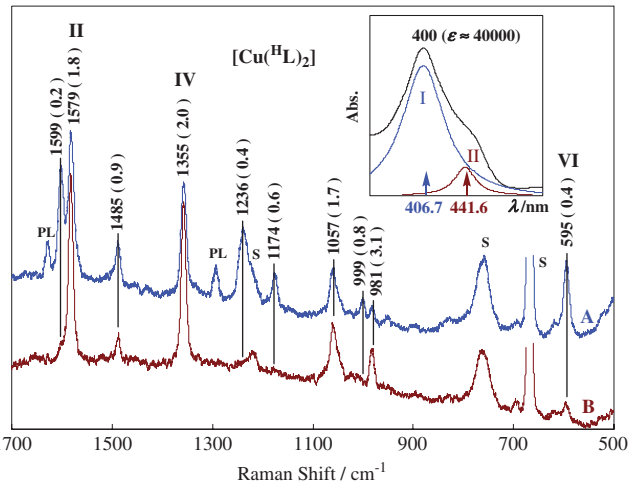

Figure 4. RR spectra of $[Cu(^{H}L)_2]$ in $CHCl_3$ obtained in the 500–1700 cm^{-1} region using 406.7 nm excitation, 7.0 mW (A) and 441.6 nm excitation, 5.9 mW (B), and 4 cm^{-1} slit widths. The sample concentration is the same for A and B. S indicates the solvent Raman band. PL indicates a spontaneous emission line. The relative intensities (441.6/406.7 nm) of Raman bands are shown in parentheses. Inset: Absorption spectrum of $[Cu(^{H}L)_2]$ in $CHCl_3$.

RR spectra are compared in Figure 3 for $[Cu(^{Me}L)_2]$ in $CHCl_3$ with different excitations of 406.7 and 441.6 nm lasers. The electronic absorption spectrum is depicted in the inset figure. The excitation wavelengths of 406.7 and 441.6 nm are matched to two divided absorption bands, Abs-band I ($[Cu(^{Me}L)_2]$) and Abs-band II ($[Cu(^{Me}L)_2]$), respectively. The crystal structure of this complex has not been solved yet, so that doubt still remains as to whether the sample is a mixture of two components, each showing Abs-band I and II. However, the observed frequencies are perfectly equal in both RR spectra. Therefore, the observed Raman spectra do not allow for the possibility of such a mixture and suggest that the sample consists of a single component with at least two absorption bands around 400 nm. It is noteworthy to mention that the Raman frequencies are comparable but the intensities depend upon the vibrational modes in the two RR spectra. The relative intensity of a Raman band (441.6/406.7 nm) is shown in parentheses on the band when the spectra are normalized using a solvent band at 760 cm^{-1}. Upon 441.6 nm excitation, resonance-enhanced Raman bands II (1587 cm^{-1}) and IV (1365 cm^{-1}) are seen, whereas Raman bands V (1260 cm^{-1}) and VI (596 cm^{-1}) are de-enhanced with excitation using 441.6 nm laser. It is obvious that the spectral pattern, which is resonant for Abs-band II, is very similar to that measured for the complexes belonging to group B with excitation of a 406.7 nm laser. Therefore, it is deduced that Abs-band II seems to have the same electronic properties as the single absorption band for the complexes belonging to group B. It should be added that the intensities of the Raman bands at 1028 and 972 cm^{-1} are resonance-enhanced and bands at 1167 and 998 cm^{-1} for $[Cu(^{Me}L)_2]$ are de-enhanced with excitation using the 441.6 nm laser. In particular, it is interesting that the band at 1167 cm^{-1} assigned mainly to the C_α–Me stretching is intensified with excitation within Abs-band I.

The RR spectra of another group A complex, $[Cu(^{H}L)_2]$ in $CHCl_3$, are also compared upon different excitations in Figure 4. The electronic absorption spectrum is depicted in the inset figure. The excitation wavelengths of 406.7 and 441.6 nm are matched to two divided absorption bands, Abs-band I ($[Cu(^{H}L)_2]$) and Abs-band II ($[Cu(^{H}L)_2]$), respectively, where the fraction of Abs-band II with respect to the whole spectrum is much less than that in the case of $[Cu(^{Me}L)_2]$. The observed Raman frequencies are perfectly equal for both RR spectra. The relative intensity of a Raman band (441.6/406.7 nm) is shown in parentheses on the band when the spectra are normalized using a solvent band at 760 cm^{-1}. Upon 441.6 nm excitation, resonance-enhanced Raman bands II (1579 cm^{-1}) and IV (1355 cm^{-1}) are seen, whereas Raman bands I (1599 cm^{-1}), V (1236 cm^{-1}), and VI (595 cm^{-1}) are de-enhanced with 441.6 nm laser excitation. It is obvious that the spectral pattern which is resonant for Abs-band II is very similar to that measured for the complexes belonging to group B with 406.7 nm laser excitation, as already pointed out in the case of $[Cu(^{Me}L)_2]$. It should be added that the intensities of the Raman bands at 1057 and 981 cm^{-1} are resonance-enhanced and bands at 1174 and 999 cm^{-1} are de-enhanced with 441.6 nm laser excitation.

Detailed resonance Raman excitation profile is a unique probe to study the structure of a molecule in electronic excited states.[2,9] Even RR spectra obtained with only two different excitation wavelengths can sometimes elucidate the nature of electronic transitions and electronic excited states. Our observation for the complexes belonging to group A is such a case, as shown in Figures 3 and 4. The absorption spectrum and the energy diagram for $[Cu(^{Me}L)_2]$ is illustrated schematically with related RR vibrational modes in Figure 5. The Raman band II is resonance-enhanced upon 441.6 nm excitation for which the $\nu(C_\beta$–N) mode dominates. It turns out that Raman band II

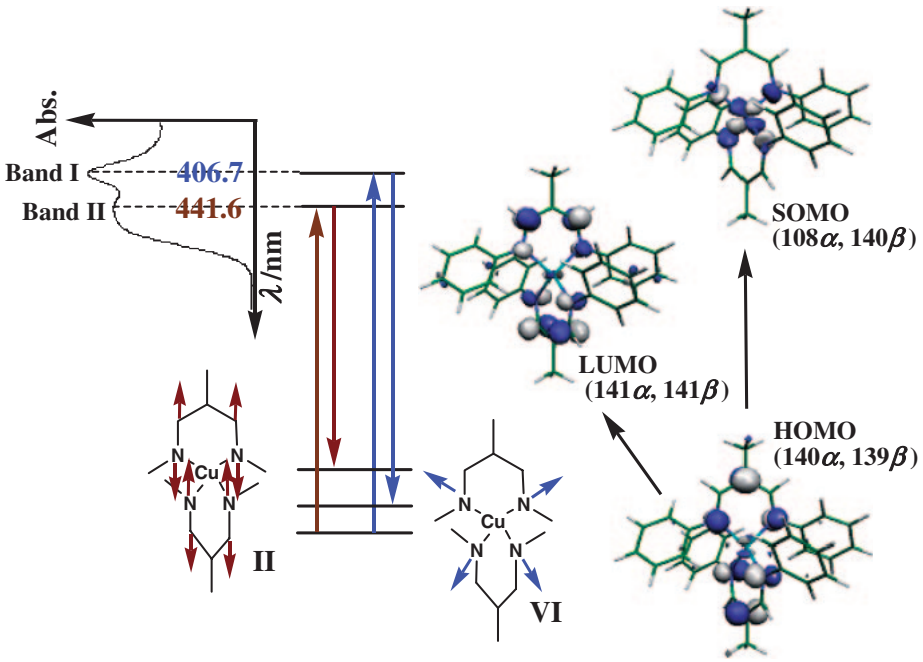

Figure 5. Absorption spectrum and energy diagram of $[Cu(^{Me}L)_2]$ related to the $\pi^* \leftarrow \pi$ electronic transitions around 400 nm. See text for details.

gains intensity effectively when the electronic excited state is distorted in the direction of the C_β–N bond. Therefore, it is deduced that the position of the potential minimum shifts along the C_β–N bond in the electronic excited state associated with Abs-band II. In contrast, Raman band VI of $[Cu(^{Me}L)_2]$ is obviously intensified in the RR spectra excited within Abs-band I for which the ν(Cu–N) mode dominates. A similar consideration as mentioned for the $\nu(C_\beta\text{–}N)$ mode leads to the idea that the core surrounded by four nitrogen atoms expands in the direction of the Cu–N bond in the electronic excited state of Abs-band I as shown in Figure 5. Consequently, the RR observations suggest that the bond lengths of Cu–N and C_β–N in the copper(II) complexes belonging to group A are elongated in the electronic excited states associated with Abs-band I and Abs-band II, respectively. These deductions concerning the electronic states are consistent with theoretical calculations and pave the way for investigations of the electronic excited states in future studies. According to MO calculations for $[Cu(^{Me}L)_2]$, the doubly-occupied HOMO (140α, 139β) and the singly-occupied SOMO (108α, 140β) consist of a π orbital of the ligand and the d_{xy}-N lone pair (z is defined as the direction of bisecting the larger angles consisting of two ligand planes), respectively, and the LUMO (141α, 141β) consists of the π^* orbital of the ligand which is antibonding, especially for the $\pi(C_\beta\text{–}N)$ bond, as shown in Figure 5.[10] One electron transition from $\psi(140\alpha)$ to $\psi(141\alpha)$ appears to correspond to Abs-band II and a transition from $\psi(139\beta)$ to $\psi(140\beta)$ corresponds to Abs-band I, which is consistent with the Raman band behavior mentioned above. Therefore, it is concluded that each complex belonging to group B has an absorption band due to the $\pi^* \leftarrow \pi$ transition while each complex belonging to group A has an extra absorption band due to LMCT transition (Abs-band I) around 400 nm in addition to the $\pi^* \leftarrow \pi$ transition band (Abs-band II) which is common to all four copper(II) complexes. Based on the RR excitation profile, we can summarize that the electronic absorption band with a common property shows a longer wavelength shift from 370, 388 nm to 445, 450 nm (not from 370, 388 nm to 400, 410 nm) as electron-donation of the substituents increases in the order of $NO_2 < CN < H < Me$, and Abs-band I is observed at 400 nm for $[Cu(^{H}L)_2]$ and at 410 nm for $[Cu(^{Me}L)_2]$ which is not observed for the complexes of group B.

The RR spectra of the complexes were measured in different solvents in order to evaluate the solvent effects that could be the cause of frequency discrepancies between the calculations and the experiments. Solvent dependency is observed only for $[Cu(^{NO_2}L)_2]$. The absorption maximum shifts to a longer wavelength by 4 nm in $CHCl_3$ from the maximum at 366 nm in THF, and the RR spectra in both THF and $CHCl_3$ are shown in Figure 6. A combination band of NO_2 symmetric stretching and C_α–NO_2 stretching at 1101 cm^{-1} in $CHCl_3$ shows a shift of 6 cm^{-1} and Raman bands III and IV also shift only a several frequencies. There are almost no frequency shifts for vibrations relevant to NO_2 substituents (769–769 cm^{-1} for NO_2 scissors, 857–856 cm^{-1} for NO_2 scissors, and 1298–1300 cm^{-1} for NO_2 asymmetric stretching) which involve substantial discrepancies in their frequencies between observed and calculated values shown as $\Delta = \nu_{obs} - \nu_{calc}$ in Table 1. Thus, solvent effects are not associated with the discrepancy.

It is intriguing that some prominent intensity changes are observed when the solvent is changed. The Raman bands observed at 769, 856, and 1101 cm^{-1} (after subtraction of the contribution of the overlapped solvent band) are intensified by roughly 3 times in $CHCl_3$. Raman band II (1587 cm^{-1} in $CHCl_3$) is used as an intensity standard band that involves neither $\nu(C_\alpha\text{–}NO_2)$ nor internal vibrations of NO_2 and shows no frequency shift in different solvents. However, an asymmetric

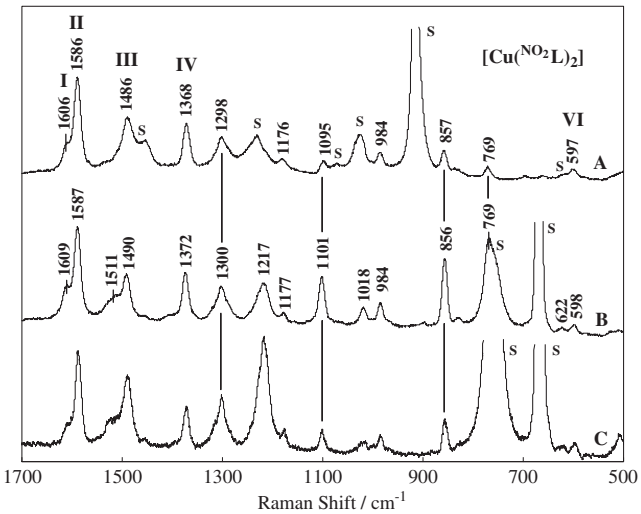

Figure 6. RR spectra of $[Cu(^{NO_2}L)_2]$ in THF (A) and in $CHCl_3$ (B) obtained in the 500–1700 cm^{-1} region using 406.7 nm excitation, 7.0 mW, and in $CHCl_3$ using 441.6 nm exicitation, 9.7 mW (C).

Raman band at 1300 cm^{-1} shows almost no intensity change. The electronic absorption maximum of $[Cu(^{NO_2}L)_2]$ shows an up-shift from 366 nm in THF to 370 nm in $CHCl_3$. This shift implies that the molecular structure should change little in the electronic ground state but should change significantly in the electronic excited state with changing of solvents because of the experimental facts of few frequency shifts and evident intensity changes of some Raman bands. The Raman bands at 1101, 856, and 769 cm^{-1} in Figure 6B are assigned to symmetric displacements of atoms belonging to substituents NO_2 so that the resonance Raman enhancement mechanism is understood as the Albrecht *A*-term,[11] in which symmetric structural changes are induced for N–O distances in $CHCl_3$ in the electronic excited state. The complex shows very weak absorption bands at 450 nm in $CHCl_3$ and the RR spectrum excited at 441.6 nm is measured, illustrated in Figure 6C. The intensity of Raman band II at 1587 cm^{-1} is normalized to that of the complex excited at 406.7 nm in $CHCl_3$. The intensities are reduced dramatically for Raman bands assigned to *a* modes of NO_2 symmetric stretching (bands at 1101 and 856 cm^{-1}, but the band at 769 cm^{-1} could not be evaluated because of overlap with the strong solvent Raman band), while the b_2 mode at 1300 cm^{-1} is at least intensified due to NO_2 asymmetric stretching. It seems that the asymmetric vibrational mode couples the weak absorption band at 450 nm to the intense absorption band at 370 nm and borrows intensity through the Albrecht *B*-term[11] resonance Raman mechanism in $CHCl_3$.

Summary

The absorption maxima around the visible-to-UV region in $[Cu(^{R}L)_2]$ (R = Me, H, CN, and NO_2) shift to longer wavelengths as the electron-donating ability of the substituents increases and an extra absorption band is observed for $[Cu(^{Me}L)_2]$ and $[Cu(^{H}L)_2]$. We have evaluated the resonance Raman spectra of these complexes with the aid of vibrational frequency calculations in order to elucidate molecular structures and electronic absorption bands in solution.

All of the RR spectra excited at 406.7 nm have corresponding Raman bands in common and the complexes can be comprised to two groups in terms of resonance enhancement patterns for the Raman bands, group A consisting of a member of $[Cu(^{Me}L)_2]$ and $[Cu(^{H}L)_2]$, and group B of $[Cu(^{CN}L)_2]$ and $[Cu(^{NO_2}L)_2]$. The RR spectra of the group A complexes are also measured with the 441.6 nm laser which is resonant to Abs-band II. The RR observations suggest that the bond lengths of Cu–N and C_β–N in the copper(II) complexes belonging to group A are elongated in the electronic excited states associated with Abs-band I and Abs-band II, respectively. Consequently, it is concluded that the Abs-band II in group A correspond to the single absorption band in complexes belonging to group B, which is the $\pi^* \leftarrow \pi$ transition and the Abs-band I in group A is assigned to LMCT transition, which is not seen in group B.

Experimental

The copper(II) complexes, $[Cu(^{Me}L)_2]$, $[Cu(^{H}L)_2]$, $[Cu(^{CN}L)_2]$, and $[Cu(^{NO_2}L)_2]$, used for the present study were synthesized in accordance with published procedures.[5] The elemental analyses data are shown in the literature.[5] Electronic absorption spectra (U-3000 spectrometer, Hitachi) were measured using a 1 mm path length cuvette. Raman scattering was excited by a Kr^+ laser (Model 2580, Spectra Physics) or He/Cd laser (CDR80SG, Kimmon Koha Co., Ltd.) and recorded using a Raman spectrometer (400D, JEOL).

Ab initio calculations for the complexes based on DFT with B3LYP functional[12,13] were performed using the Gaussian 03 program package[14] with the 6-31G basis set.[15] All geometries were fully optimized at that level. A correction of the calculated frequencies to those observed was made using a scaling factor of 0.9582 that modified a single global scaling factor of 0.9613[16] employed for the 6-31G(d) basis set. The new scaling factor is derived as follows. First, normal mode calculations were carried out by using both basis functions 6-31G and 6-31G(d) for a structurally simplified complex $[Cu(^{H}L')_2]$ wherein 4 phenyl substituents in two L are all replaced by a hydrogen atom. Next, a correction factor α was obtained for each vibrational mode ν_a calculated as $\alpha\nu_a(\text{6-31G}) = \nu_a(\text{6-31G(d)})$ for different bases functions. Calculating the mean α over all vibrational modes generates a value of 0.9968 and then a new scaling factor is obtained as $0.9582 = 0.9968 \times 0.9613$. Vibrational correlations for each vibrational mode in different complexes were estimated by taking the dot products (overlap) of every combination of normal modes of four different substituted complexes.[17,18]

References

1 L. Bourget-Merle, M. F. Lappert, J. R. Severn, *Chem. Rev.* **2002**, *102*, 3031.

2 P. L. Holland, C. J. Cramer, E. C. Wilkinson, S. Mahapatra, K. R. Rodgers, S. Itoh, M. Taki, S. Fukuzumi, L. Que, Jr., W. B. Tolman, *J. Am. Chem. Soc.* **2000**, *122*, 792.

3 S. D. Allen, D. R. Moore, E. B. Lobkovsky, G. W. Coates, *J. Am. Chem. Soc.* **2002**, *124*, 14284.

4 S. Yokota, Y. Tachi, N. Nishiwaki, M. Ariga, S. Itoh, *Inorg. Chem.* **2001**, *40*, 5316.

5 C. Shimokawa, S. Yokota, Y. Tachi, N. Nishiwaki, M.

Ariga, S. Itoh, *Inorg. Chem.* **2003**, *42*, 8395.

6 C. Shimokawa, J. Teraoka, Y. Tachi, S. Itoh, *J. Inorg. Biochem.* **2006**, *100*, 1118.

7 T. Osako, S. Nagatomo, Y. Tachi, T. Kitagawa, S. Itoh, *Angew. Chem., Int. Ed.* **2002**, *41*, 4325.

8 S. Mahapatra, J. A. Halfen, E. C. Wilkinson, G. Pan, X. Wang, V. G. Young, Jr., C. J. Cramer, L. Que, Jr., W. B. Tolman, *J. Am. Chem. Soc.* **1996**, *118*, 11555.

9 M. J. Henson, P. Mukherjee, D. E. Root, T. D. P. Stack, E. I. Solomon, *J. Am. Chem. Soc.* **1999**, *121*, 10332.

10 P. Flukiger, H. P. Luthi, S. Portmann, J. Weber, *MOLEKEL 4.0*, Swiss Center for Scientific Computing, Manno, Switzerland, **2000**.

11 A. C. Albrecht, *J. Chem. Phys.* **1961**, *34*, 1476.

12 C. Lee, W. Yang, R. G. Parr, *Phys. Rev. B* **1988**, *37*, 785.

13 A. D. Becke, *J. Chem. Phys.* **1993**, *98*, 5648.

14 M. J. Frisch, G. W. Trucks, H. B. Schlegel, G. E. Scuseria, M. A. Robb, J. R. Cheeseman, V. G. Zakrzewski, J. A. Montgomery, Jr., R. E. Stratmann, J. C. Burant, S. Dapprich, J. M. Millam, A. D. Daniels, K. N. Kudin, M. C. Strain, O. Farkas, J. Tomasi, V. Barone, M. Cossi, R. Cammi, B. Mennucci, C. Pomelli, C. Adamo, S. Clifford, J. Ochterski, G. A. Petersson, P. Y. Ayala, Q. Cui, K. Morokuma, D. K. Malick, A. D. Rabuck, K. Raghavachari, J. B. Foresman, J. Cioslowski, J. V. Ortiz, A. G. Baboul, B. B. Stefanov, G. Liu, A. Liashenko, P. Piskorz, I. Komaromi, R. Gomperts, R. L. Martin, D. F. Fox, T. Keith, M. A. AlLaham, C. Y. Peng, A. Nanayakkara, M. Challacombe, P. M. W. Gill, B. Johnson, W. Chen, M. W. Wong, J. L. Andres, C. Gonzalez, M. Head-Gordon, E. S. Replogle, J. A. Pople, *Gaussian98*, Gaussian, Inc., Pittsburgh, PA, **1998**.

15 R. Ditchfield, W. J. Hehre, J. A. Pople, *J. Chem. Phys.* **1971**, *54*, 724.

16 G. Rauhut, P. Pulay, *J. Phys. Chem.* **1995**, *99*, 3093.

17 R. M. Gulam, T. Matsushita, S. Neya, N. Funasaki, J. Teraoka, *Chem. Phys. Lett.* **2002**, *357*, 126.

18 R. M. Gulam, T. Matsushita, J. Teraoka, *J. Phys. Chem. A* **2003**, *107*, 2172.